Dark sector searches at Belle II

L. Corona *†
INFN Sezione di Pisa, 56127 Pisa, Italy

Abstract

Belle II has unique reach for a broad class of models that postulate the existence of dark matter particles with MeV–GeV masses. In this manuscript, we present recent world-leading physics results from Belle II searches for Z′ bosons, axion-like particles, and dark scalars in association with two muons in e^+e^- collisions; invisible particles produced in decays of τ leptons; long-lived (pseudo)scalars produced in decays of β mesons; inelastic dark matter; and the near-term prospects for other dark sector searches.

Keywords: High Energy Physics, Dark Sector, Dark Matter, Belle II, B-factory, SuperKEKB
DOI: 10.31526/PHEP.2025.04

1. INTRODUCTION

Several astrophysical observations suggest the existence of dark matter (DM), a component of matter that does not interact through strong or electromagnetic forces. Although DM constitutes approximately 85% of the total matter in our Universe, its nature remains unknown. For this reason, DM is one of the most compelling phenomena in support for physics beyond the Standard Model (SM). If DM consists of particles feebly coupled with SM particles, it could be produced in SM particle annihilations at high-energy colliders. The lack of evidence of non-SM physics at the electroweak scale leads to hypothesize sub-GeV DM particles feebly interacting with SM particles through non-SM mediators. Sub-GeV DM and the non-SM mediators belong to the dark sector, and efforts to detect them have been actively pursued at beam dump and high-intensity frontier experiments. Belle II [1, 3] is a high-intensity frontier experiment that operates at the SuperKEKB e^+e^- asymmetric-energy collider [2]. During the first data taking run (2019–2022), Belle II collected a sample of e^+e^- collision data corresponding to 427 fb^{-1} of integrated luminosity. From June 2022 to January 2024, there was a period of long shutdown of the experiment dedicated to maintenance and upgrades of both the SuperKEKB accelerator and the Belle II detector. On January 2024, the second data taking period has started, and Belle II collected an additional data sample of about 150 fb^{-1} . Since the beginning of data taking in 2019, Belle II has collected a dataset corresponding to $575 fb^{-1}$ of integrated luminosity, of which 490 fb^{-1} have been collected at a center-of-mass energy $\sqrt{s}$= 10.58 GeV, where pairs of B mesons are produced at threshold. Thanks to the excellent reconstruction capabilities for low multiplicity and missing energy signatures, and dedicated triggers, Belle II has a unique or world-leading sensitivity to dark sector particles with a mass in the MeV–GeV range [4].

†Corresponding author:luigi.corona@pi.infn.it
†on behalf of the Belle II Collaboration

2. RECENT DARK SECTOR RESULTS AT BELLE II

Extensions of the SM predict several experimental signatures that depend on the relation between the masses of an hypothetical DM candidate and a dark sector mediator. If a DM candidate exists and it is heavier than the dark sector mediator, the latter could decay to SM particles that can be detected in the experiments. If the mass of the dark sector mediator is sufficiently greater than the mass of the DM candidate, the decay of the dark sector mediator to DM would be favored. The DM would have a negligible interaction with the detector, so the decays of the dark sector mediators to DM particles lead to missing energy signatures. Finally, in models where the mediators could decay to SM particles but the decay is suppressed, the dark sector mediators could be naturally long-lived leading to signatures with displaced vertices. Belle II has a unique sensitivity to all these signatures, and we present here the latest results on dark sector searches performed at Belle II.

2.1. Search for an invisible Z′

The $L_\mu - L_\tau$ model [5, 6, 7] introduces a light gauge boson, Z′ , that violates lepton-flavor universality while conserving the difference between μ and τ lepton numbers. We search for the invisible decay of the Z′ through the process $e^+e^- \to \mu^+\mu^- Z'(\to inv.)$, where the Z' is radiated off one of the muons. The Z′ could decay invisibly to SM neutrinos, with a branching fraction ranging in B $(Z' \to inv.)100\% - 33\%$ depending on the Z' mass, as predicted by the $L_\mu - L_\tau$ model, or to kinematically accessible DM candidates with a branching ratio of $B(Z' \to inv.)$= 100%. A signal would appear as a narrow enhancement in the recoil mass computed against the two final-state muons, in events where nothing else is detected. The main SM backgrounds are the following: $e^+e^- \to \mu^+\mu^-(\gamma)$, where the photon γ is not detected; $e^+e^- \to \tau^+\tau^-(\gamma)$, where the missing energy is due to neutrinos; and $e^+e^- \to e^+e^-\mu^+\mu^-$ where the electron and positron in the final state escape the detection. The $e^+e^- \to e^+e^-\mu^+\mu^-$ events contribute mostly for recoil masses greater than 7 GeV/c^2 , while $e^+e^- \to \mu^+\mu^-(\gamma)$ contributes mostly for recoil masses below $2GeV/c^2$. The $e^+e^- \to \tau^+\tau^-$ events are the main contribution to background elsewhere. The SM backgrounds are suppressed using a neural-network trained simultaneously for all Z′ masses [8], and fed with kinematic variables sensitive to the origin of the missing energy: in the signal, the Z′ is produced as final-state radiation (FSR); in the background, the missing energy is due to neutrinos or un-

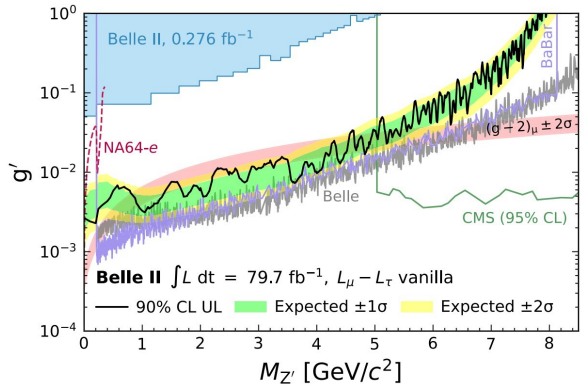

FIGURE 1: Observed 90% CL upper limits and corresponding expected limits on the Z coupling as a function of the Z mass, assuming the branching ratios predicted by the $L_\mu - L_\tau$ model.

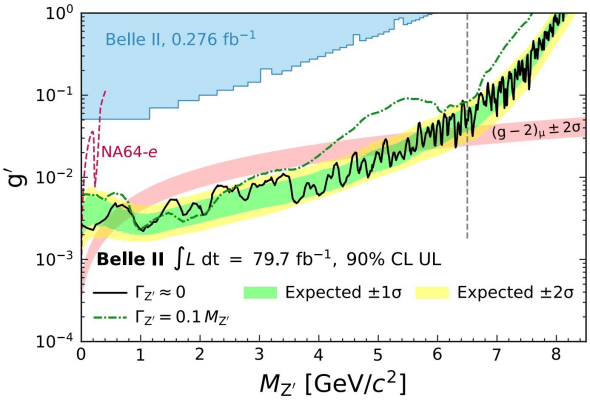

FIGURE 2: Observed 90% CL upper limits and corresponding expected limits on the Z′ coupling as a function of the Z mass, assuming$B(Z' \to inv.) = 100\%$

detected particles. The signal efficiency is typically 5%. The main systematic uncertainties are from data-simulation comparison, ranging in 15%–35%. From 2D template fits to the recoil mass squared, in bins of the recoil polar angle, we do not observe any significant excess in 79.7fb^{-1} of data, and we set 90% C.L. upper limits on the cross section of the process as small as 0.2 fb. Limits are mainly affected by statistical uncertainties for m'_z <6 GeV/c^2 , and systematic uncertainties affect them by less than 5%. Above 6 GeV/C^2 limits are dominated by systematic uncertainties, degrading them by 40%. We translate the limits on the cross section into 90% limits on the coupling of the $L_\mu - L_\tau$ model, g′ , as a function of the Z' mass, m'_Z. We exclude the region favored by the $(g2)_\mu$ anomaly [9], which could be explained by the $L_\mu - L_\tau$ model, in the mass range 0.8 <m$'_Z$ < 5 GeV/C^2

for the fully invisible $L_\mu - L_\tau$ model. Fig. 1 shows the results obtained assuming the branching ratios predicted by the $L_\mu - L_\tau$ model, while Fig. 2 shows the results obtained assuming B (Z′ → inv.) = 100% [10, 11].

2.2. *Search for* $e^+e^- \to \mu^+\mu X(\to \tau^+\tau^-)$

We search for a$X \to \mu^+\mu^-\tau^+\tau^-$ resonance, where$X$ could be a Z′ from the $L_\mu - L_\nu$ model, a leptophilic dark scalar S, or an axion-like particle (ALP), in $e^+e^- \to \mu^+\mu^-$ events, with τ decaying to one charged particle. The S is a Higgs-like spin-0 hypothetical particle that couples preferentially to charged leptons through Yukawa-like couplings [12]. Axion-like particles are pseudoscalars that appear in many SM extensions [13, 14]. Similarly to the $Z' \to inv.$ analysis, we search for a narrow enhancement in the recoil mass against two oppositely charged muons, in four track events with zero net charge. The main SM backgrounds are QED radiative dilepton, four lepton final-state processes, and $e^+e^- \to q\bar{q}(\gamma)$ events. Standard Model backgrounds are suppressed with eight neural-networks fed with kinematic variables sensitive to the X-production mechanism as FSR off one of the tw omuons,and trained in different X-mass regions. The signal efficiency ranges from 12% for the X-mass at the kinematic threshold to 2% for a X-mass of 10 GeV/c^2. After the background suppression, we observe large data simulation discrepancy due to missing effect in simulation and non-simulated processes. In particular, for recoil masses below 6 GeV/c^2, the main contribution to the discrepancy is due to the missing initial-state radiation effects in the sim ulation of four-lepton final-state process; while for masses above 6 GeV/c^2 the main contribution to the discrepancy is due to two-photon process $e^+e^- \to e^+e^-h$, where h is typically a low-mass hadronic system, which is missing in the simula tion. Despite the data-simulation discrepancy, the backgrounds are smooth on the scale of the signal resolution, which is ≈10 MeV, thus they do not mimic the signal. To minimize the impact of not correctly simulated background, the signal and background yields are directly measured on data. Progress in High Energy Physics The main systematic uncertainty comes from particle identification efficiency differences in data and simulation. The total systematic uncertainty is ≈ 10% From extended maximum likelihood fits to the recoil mass distribution, we do not observe any significant excess in 62.8 fb^1 of data. We derive 90% C.L. upper limits on the cross section of the process, $\sigma(e^+e^- \to \mu^+\mu^-) \times \beta(X \to \tau^+\tau^-)$, that range from 0.7 fb to 24 fb. We reinterpret the upper limits on the cross sections in the three different dark sector models considered. We ob tain world-leading 90% C.L. upper limits on the S-coupling ζ for $m_S > 6.5\ GeV/c^2$, and on the ALP-lepton coupling $|C_{ll}|/\Lambda$, in the entire mass range $3.6 < m_{ALP} < 10\ GeV/c^2$, assuming equal ALP-couplings to the three lepton families and zero couplings to all other particles [15]. For the reinterpretation, we evaluated the signal effi ciency of the analysis in all the models considered without observing significant differences. Fig. 3 and Fig. 4 show the results obtained for the lep tophilic dark scalar and for the ALP, respectively

2.3. *Search for* $e^+e \to \mu^+\mu X(\to \mu^+\mu)$

We search for an $X \to \mu^+\mu^-$ resonance in $e^+e^- \to \mu^+\mu^-\mu^+\mu^-$ events as a narrow enhancement in the dimuon mass distribution in four-track events with zero net charge and no extra energy. The X resonance could be a Z' predicted by the $L_\mu - L_\tau$ model, or a muonphilic scalar S, which is a spin-0 boson that couples exclusively to muons through a Yukawa-like interaction. The dominant background is the SM four-muon final-state process. Background is suppressed by applying five neural networks trained on kinematic variables sensitive to the X-production mechanism, such as final-state radiation (FSR) off one of the two muons, and the presence of a resonance in both the candidate and the recoil muon

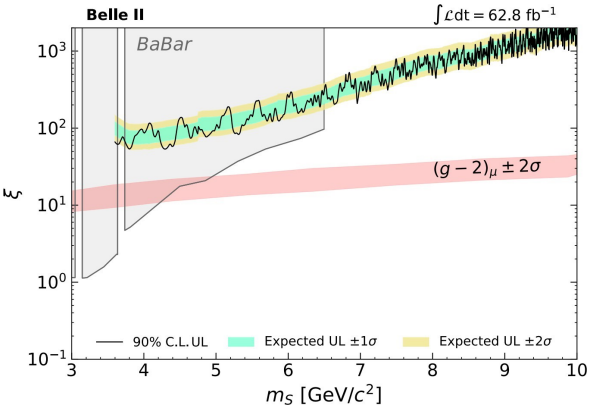

FIGURE 3: Observed 90% CL upper limits (UL) and corresponding expected limits as a function of the mass on the leptophilic scalar coupling ζ

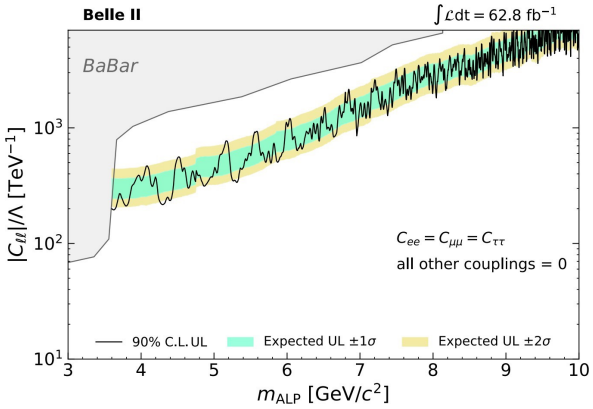

FIGURE 4: Observed 90% CL upper limits (UL) and corresponding expected limits as a function of the mass on the ALP-lepton coupling C_{ll}/Λ.

pairs, trained in different X-mass ranges. The signal efficiency for the muonphilic scalar is generally smaller than in the Z' case for masses above 1 GeV/c^2, ranging from 15%–25% and 25%–35% respectively. In particular, for recoil masses below 6 GeV/c^2, the analysis is optimized for the Z' case. The main contribution to the discrepancy is due to the missing initial-state radiation effects in the simulation of the four-lepton final-state process, while for masses above 6 GeV/c^2, the main contribution is due to the two-photon process $e^+e^- \to e^+e^-h$, where h is typically a low-mass hadronic system, which is not included in the simulation. Despite the data-simulation discrepancy, the backgrounds are smooth on the scale of the signal resolution (10 MeV); thus, they do not mimic the signal. To minimize the impact of incorrectly simulated background, the signal and background yields are directly measured on data. The muonphilic scalar is produced through a p-wave process due to angular momentum conservation and has a higher momentum spectrum than the Z', which is produced via an s-wave. This implies the presence of a higher-momentum muon, which is better identified and reconstructed. For masses below 1 GeV/c^2, this results in a higher efficiency of 35% for the muonphilic scalar, compared to 25% for the Z'. The main contribution to the systematic uncertainty comes from the neural-network selections. The total systematic uncertainty ranges from 9.5% to 13%, depending on the mass. From extended maximum likelihood fits to the dimuon mass distribution, we do not observe any significant excess in 178 fb^{-1} of data, and we set 90% CL upper limits on the cross section of the process, ranging from 0.046 fb to 0.97 fb for the Z′ model and from 0.055 fb to 1.3 fb for the muonphilic scalar model. We interpret the results obtained on the cross section as 90%CL limits on the Z′ coupling of the $L_\mu - L_\tau$ model and on the coupling of a muonphilic scalar S with muons [16]. Despite the small dataset used, we obtain similar results with the existing limits on Z′ from BABAR [17] and Belle [18], which performed the analysis with 514 fb^{-1} and 643 fb^{-1}, respectively. We set the first limits for the muonphilic scalar model from a dedicated search. Figures 5 and 6 show the results obtained for the Z′ the $L_\mu - L_\tau$ model, and for the muonphilic scalar model respectively .

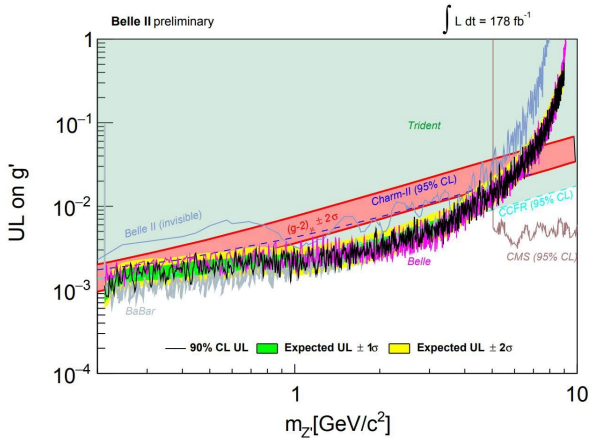

FIGURE 5: Observed 90% CL upper limits and corresponding expected limits as a function of the mass on the Z′ coupling of the $L_\mu - L_\tau$ model

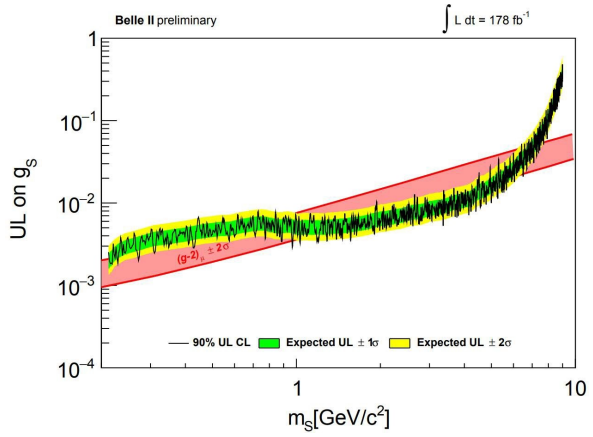

FIGURE 6: Observed 90% CL upper limits and corresponding expected limits as a function of the mass on the muonphilic dark scalar model.

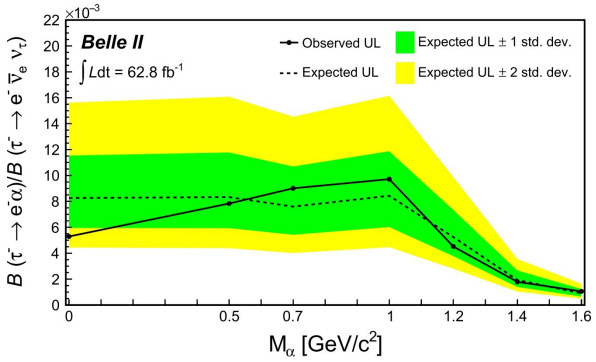

FIGURE 7: Upper limits at 95% C.L. on the ratio $\beta(\tau \to e\alpha)/\beta(\tau \to e\bar{\nu}_e\nu_\tau)$

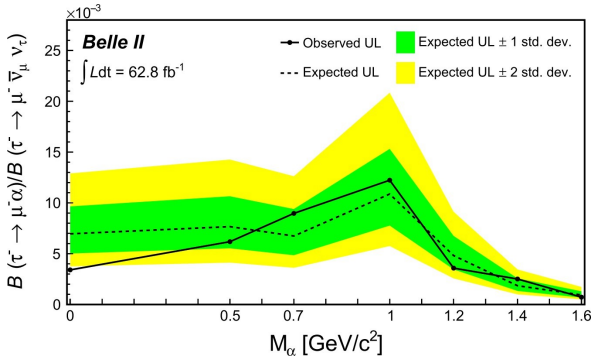

FIGURE 8: Upper limits at 95% C.L. on the ratio $\beta(\tau \to \mu\alpha)/\beta(\tau \to \mu\bar{\nu}_\mu\nu_\tau)$

2.4. *Search for the $\tau \to l\alpha$ decay*

Charged-lepton flavour violation (LFV) is allowed in various extensions of the SM, however it has never been observed. In these extensions, the LFV processes could be mediated by a new hypothetical α spin-0 boson. We search for an invisibleα produced in the$\tau \to l\alpha$ decay, with $l = e, \mu$, in $e^+e^- \to \tau^+\tau^-$ events. We use a sample of 57.7 million $e^+e^- \to \tau^+\tau^-$ events,corresponding to an integrated luminosity of 62.8 fb^{-1}. In the center of-mass frame, τ pairs are produced back-to-back so that the decay products of each τ lepton are contained in two separate hemispheres. The tag hemisphere contains three charged hadrons from $\tau^-_{tag} \to h{-}h^+h^-\nu_\tau$ while the signal hemisphere contains only one charged lepton with $h = \pi, K$ while the signal hemisphere contains only one charged lepton from the $\tau^-_{sig} \to l^-\alpha$-decay

For this analysis, $\tau \to l\nu_\tau\bar{\nu}_l$is an irreducible background. However, the lepton momentum has a broad distribution for the background, while it depends only on the α mass for the signal and it appears as a bump over the irreducible back ground. In particular, we search for an excess over the normalized lepton energy spectrum x_l of $\tau \to l\nu_\tau\bar{\nu}_l$, where $x_l = 2E^\star_l/m_\tau$, performing template fits. The energy $E^\star_l$ is defined in the approximate rest frame of τ_{sig}, i.e. where $E_\tau = \sqrt{s}/2$ and $\sqrt{s}$is the energy in the center of-mass frame, and the τ_{sig} direction is opposite to the τ_{tag} direction. The signal efficiency de pends on the $\alpha - mass$: it varies between 9.4% and 13.9% for the $\tau^- \to e^-\alpha$ decays, and be tween 9.1% and 17.4% for the $\tau^- \to \mu^-\alpha$ decays. The main systematic uncertainties originate from lepton-identification efficiency and particle misidentification rate, based on data-simulation comparison. We do not find any significant excess in 62.8 fb^{-1} of data, and we set world-leading 95C.L. upper limits to $\beta(\tau \to l\alpha)/\beta(\tau \to l\bar{\nu}_l\nu_\tau)$, as a function of the M_α mass[19]. Theupperlim its range in 1.1–9.7 $\times 10^{-3}$ for the electron channel and in 0.7–12.2 $\times 10^3$ for the muon channel. Systematic uncertainties degrade on average our upper limit sensitivity by approximately 35% in both channels. Results are shown in Fig. 7 and Fig. 8.

2.5. *Search for a long-lived (pseudo)scalar in $b \to s$ transition*

Some extensions of the SM introduce a new light scalar S that may give mass to DM particles. The scalar S would mix with the SM Higgs boson through a mixing angle θ, and would be naturally long-lived for small values of θ. We search for $B^0 \to K^{\star 0}(\to K^\star\pi^-)S$ and $B^+ \to K^+S$ events, with $S \to x^+x^-(x = e, \mu, \pi, K)$ forming a decay vertex displaced from the B decay vertex. We use a sample of $(198 \pm 3)10^6 B\bar{B}$ pairs, corresponding to an integrated luminosity of 189 fb^{-1}. The signal yield is extracted through extended maximum likelihood fits to the reduced invariant mass of S, $M^r_{S\to XX} = \sqrt{M^2_{S\to XX} - 4M^2_X}$, in order to im prove the modeling of the signal width close to the kinematic thresholds. The main background components are the combinatorial $e^+e^- \to q\bar{q}$, suppressed by requiring a kinematics similar to B-meson expectations; $B \to KK_S(\to \pi^+\pi^-)$, vetoed; and $B \to Kx^+x^-$ decays without inter mediate long-lived particles decaying to x^+x^-, suppressed by tightening the displacement selections. The main systematic uncertainties are as sociated with the signal efficiency and with the signal model used for the fit. The systematic un certainties on the signal efficiency are mainly due the difference in data and simulation of the track finding efficiency for displaced vertices,and range from 4%, for most of masses and lifetimes, up to 10%, for the lightest masses in the $S \to e^+e^-$ channel. The typical total uncertainty for the sig nal model is about 15% for the signal width and around 10% for the tail parameters. We do not observe any significant excess in Progress in High Energy Physics 189 fb^1 of data, and we set the first model independent limits at 95% C.L. on β(B →KS) × $\beta(S \to x^+x^-)$ as a function of the scalar mass m_s for different S-lifetimes at the level of 10^7. We reinterpret the results in the $(sin\theta, m_s)$ plane, wherethe mixing angle of S with the SM Higgs. Results are shown in Fig. 9 and Fig. 10 [20]

2.6. *Search for inelastic dark matter with a dark Higgs*

A simple non-minimal model for light dark matter introduces inelastic dark matter (IDM), where DM couples inelastically to SM particles [21]. The IDM consists of a relic DM candidate χ_1 that can be excited to a χ_2 state by absorbing a massive dark photon A'. The A′ couples to SM photon, via kinetic mixing with strength $\epsilon and to DM, with couplingg_D = \sqrt{4\pi\alpha_D}$, and decays predominantly via $A' \to \chi_1\chi_2$. For a sufficient small mass splitting $\Delta = m_{\chi 1} - m_{\chi 2}$ or a sufficient small A′ coupling, the χ_2 state results to be long-lived before decaying to χ_1 and a pair of SM particles, while χ_2 is stable and escapes the detection. To explain the A′ mass and the mass splitting Δ, the IDM model can be extended introducing a Higgs mechanism induced by a dark Higgs h′. Generally, the h′ can mix with the SM Higgs with mixing angle θ and it results to be

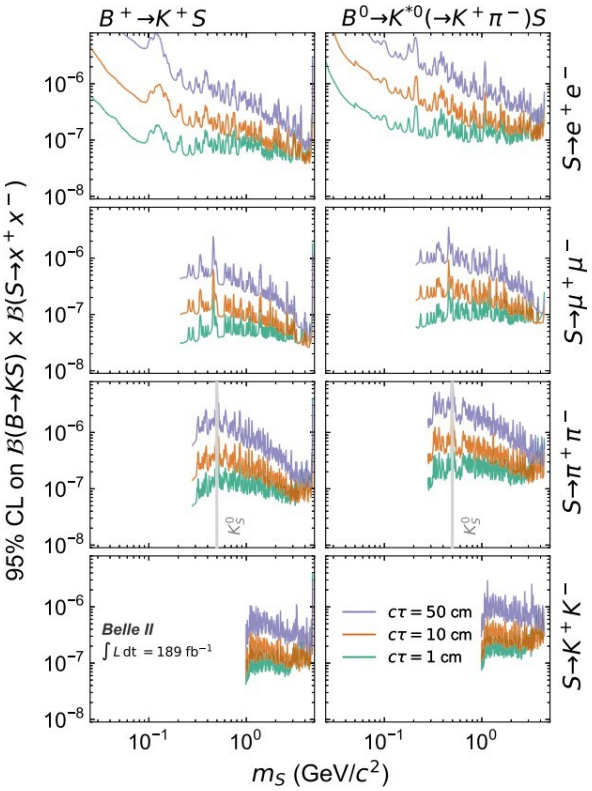

FIGURE 9: Observed 95% C.L. on $\beta(B \to KS) \times \beta(S \to x^+x^-)$ as a function of the scalar mass m_s for different lifetimes $c\tau$

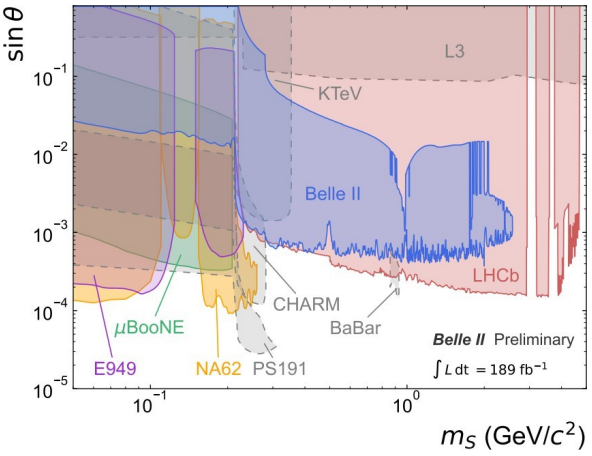

FIGURE 10: Exclusion region at 95% C.L. in the $(sin\theta, m_s)$ plane compared with existing constraints from other experiments.

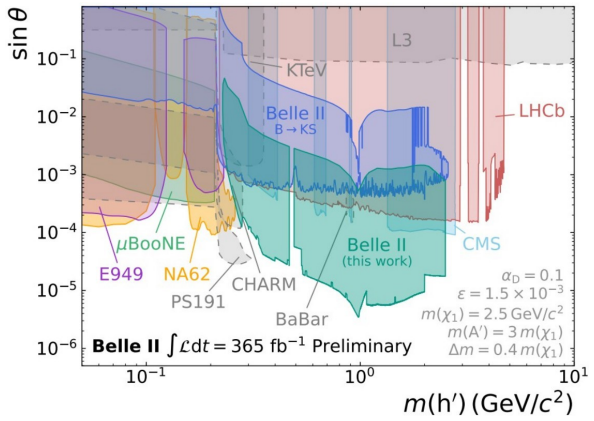

FIGURE 11: Exclusion regions at 95% C.L. in the $(sin\theta, m_{h'})$ plane compared to existing limits from other experiments, for a specific configuration of the model parameters.

naturally long lived for small values of θ. The coupling between DM and h', $\kappa \approx g_D \Delta / m'_{A'}$, depends on the other parameters of the model [22, 23]. We search for a dark Higgs boson produced in association with IDM through the process $e^+e^- \to h'(\to x^+x^-)A'(\to \chi_1\chi_2(\to \chi_1 e^+e^-))$, where $x^\pm = \mu^\pm, \pi^\pm, K^\pm$ We restrict to the case $m_{h'} < m_{\chi 1} < m_{A'}$, which allows to evade some of the existing constraints on DM. The signature consists of four tracks in the final state plus missing energy. The four tracks form up to two dis placed vertices, one pointing and the other non pointing to the interaction point (IP). In signal events, the missing energy is due to χ_1 produced in the χ_2 and A decays. A signal would appear as a narrow enhancement in the invariant mass $m(x^+x^-)$ For the analysis, we use 365 fb^1. Due to the peculiar signature, the analysis is challenging for the tracking and trigger systems but the SM background is $\approx$ *zero*. The main selections applied to reduce the SM background are the following ones: to suppress prompt SM backgrounds, we require at least one of the two vertices be displaced with a transverse distance from the IP higher than 0.2 cm; we require the h' vertex to point at the IP; to suppress background from photon conversions in the detector mate rial, we require a opening angle between the two tracks higher than 0.1 rad; to suppress SM back grounds with no missing energy associated, we require the total missing energy in the center-of mass frame to be greater then 4 GeV, i.e. two times the minimum χ_1 mass considered. We veto the regions around the K and the Λ masses in the $h' \to \pi^+\pi^-$final state to suppress back ground from K^0_S and Λ decays; we veto the region around the ϕ mass in the $h' \to K^+K^-$ final state to suppress contribution from ϕ decays produced in $e^+e^- \to \phi(\to K^+K^-)\gamma(\to e^+e^-)$. The signal efficiency varies from few percent up to 20%, depending mostly on the displacements of the h'. The main systematic uncertainties, varying from 4% to 10% depending on the f' masses and displacements, are associated to the signal efficiency. The dominant systematic uncertainty on the signal efficiency is due to data-simulation discrepancies in track finding for displaced vertices Given the small number of background events expected, we apply a counting technique to ex tract the signal. We do not observe any signif icant excess compatible with signal events, thus we set 95% C.L. upper limits on the cross section $\sigma_{sig} = \sigma(e^+e^- \to h'A'(\to \chi_1\chi_2) \times \beta(h' \to$

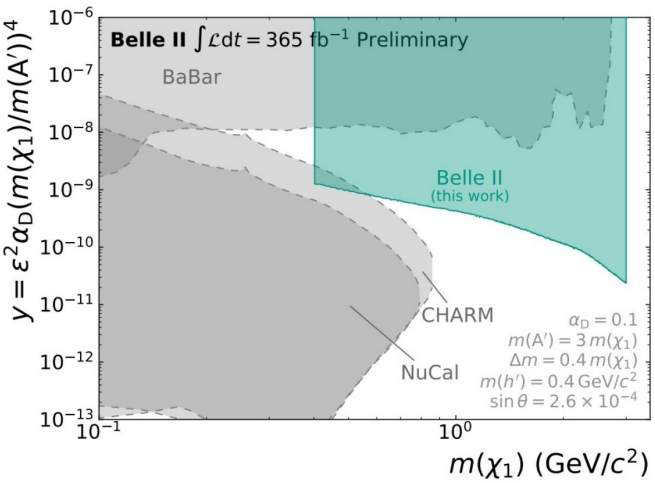

FIGURE 12: Exclusion regions at 95% C.L. in the $(y, m_{\chi 1})$ plane, where $y = \epsilon^2 \alpha_D (m_{\chi 1}/m_{A'})^4$ compared to existing limits from other experiments, for a specific configuration of the model parameters. In the y definition, ϵ is the strength of the kinetic mixing of the dark photon (A') with the SM photon, α_D is the A'-DM coupling, and $m_{\chi 1}$ and $m_{A'}$ are the masses of χ_1 and A' respectively

$x^+x^-) \times \beta(\chi_2 \to \chi_1 e^+e^-)$. We reinterpret the results obtained on the cross section as 95% C.L. limits on the $sin\theta$ as a function of the h' mass, where θ is the h'-SM Higgs mixing angle, and on the dimensionless variable$y = \epsilon^2 \alpha_D (m_{\chi 1}/m_{A'})^4$ as a function of the χ_1 , for different configurations of the model parameters. Fig. 11 and Fig. 12 show the exclusion regions at 95% C.L. in the $(sin\theta, m_{h'})$ and in the $(y, m_{\chi 1})$ planes, respectively, compared to existing limits from other experiments, for a specific configuration of the model parameters

3. SUMMARY

We presented the latest Belle II world-leading results from dark sector searches. The results use subsets of the 427 fb^{-1} collected in the first data taking run (2019–2022) at Belle II. Other Belle II results include the search for axion-like particles decaying to a two-photon fi nal state with 445 pb^{-1} collected in 2018 [24], which is in the process of being updated with the full dataset collected so far. Particularly interest ing for dark sector searches is the excess observed in $B \to K\nu\bar{\nu}$ decays at Belle II, which is 2.7 standard deviations from the Standard Model expectation [25], that could be explained by a long-lived axion-like particle; a two-body decay reinterpretation of the $B \to K\nu\bar{\nu}$ result is in progress. Newresults with improved analyses and larger data samples,including data collected during the second data taking run started in 2024, are expected to push further the Belle II sensitivity to the dark sector.

CONFLICTS OF INTEREST

The author declares that there are no conflicts of interest regarding the publication of this paper.

ACKNOWLEDGMENT

The work of S.K. and H.O. is supported in part by the Science and Technology Development Fund (STDF) Project ID 437 and the ICTP Project ID 30. The work of E.M. is supported in part by the U. S. Dept. of Energy Grant No. DE-FG03-94ER40837.

References

1] E. Kou et al. (Belle II Collaboration), Prog. Theor. Exp. Phys. 2019, 123C01 (2019).
[2] K. Akai, K. Furukawa, and H. Koiso (Su perKEKB Accelerator Team), Nucl. Instrum. Methods A 907, 188 (2018).
[3] T. Abe et al. (Belle II Collaboration), arXiv:1011.0352 [physics.ins-det] (2010).
[4] L. Aggarwal et al. (on behalf of the Belle II USgroup) arXiv:2207.06307 [hep-ex] (2022)
[5] X. G. He, G. C. Joshi, H. Lew, and R. R. Volkas, Phys. Rev. D 43, R22 (1991).
[6] B. Shuve and I. Yavin, Phys. Rev. D 89, 113004 (2014).
[7] W. Altmannshofer, S. Gori, S. Profumo, and F. S. Queiroz, J. High Energy Phys. 12, 106 (2016).
[8] F. Abudin´ en et al., Eur. Phys. J. C 82, 121 (2022).
[9] D.P. Aguillard et al. (The Muon g2 Collab oration)Phys. Rev. Lett. 131, 161802 (2023)
[10] I. Adachi et al. (Belle II Collaboration), Phys. Rev. Lett. 124, 141801 (2020).
[11] I. Adachi et al. (Belle II Collaboration), Phys. Rev. Lett. 130, 231801 (2023).
[12] B. Batell, N. Lange, D. McKeen, M. Pospelov, and A.Ritz, Phys. Rev. D95, 075003 (2017).
[13] M. Bauer, M. Neubert, and A. Thamm, J. High Energy Phys. 12 (2017) 044.
[14] M. Bauer, M. Neubert, S. Renner, M. Schnubel, and A. Thamm, J. High Energy Phys. 09 (2022) 56. [15] I.Adachietal.(BelleIICollaboration) Phys. Rev. Lett. 131, 121802 (2023).
[16] D. Forbes, C. Herwig, Y. Kahn, G Krnjaic, C. M. Suarez, N. Tran, and A. Whitbeck Phys. Rev. D 107, 116026 (2023).
[17] J. P. Lees et al. (BaBar Collaboration) Phys. Rev. D 94, 011102(R) (2016).
[18] T. Czank et al. (Belle Collaboration) Phys. Rev. D 106, 012003 (2022).
[19] I. Adachi et al. (Belle II Collaboration), Phys. Rev. Lett. 130, 181803 (2023). [20] I.Adachietal.(BelleIICollaboration) Phys. Rev. D 108, L111104 (2023).
[21] D. Tucker-Smith and N. Weiner, Phys. Rev. D64, 043502 (2001).
[22] M. Duerr et al., J. High Energ. Phys. 2020, 39 (2020).
[23] M. Duerr et al., J. High Energ. Phys. 2021, 146 (2021).
[24] F. Abudin´ en et al., Phys. Rev. Lett. 125, 161806 (2020).
[25] I. Adachi et al., Phys. Rev. D 109, 112006 (2024).